Synthesis, characterization of palygorskite supported zero-valent iron and its application for methylene blue adsorption

Ray L. Frost [a,•], Yunfei Xi [a,b,c], Hongping He [a,d]

[a] *Inorganic Materials Research Program, School of Physical and Chemical Sciences, Queensland University of Technology, GPO Box 2434, 2 George Street, Brisbane, Qld 4001, Australia;*

[b] *CERAR—Centre for Environmental Risk Assessment and Remediation, University of South Australia, Mawson Lakes, SA 5095, Australia;*

[c] *Cooperative Research Centre for Contamination Assessment and Remediation of the Environment (CRC CARE), University of South Australia, Mawson Lakes, SA 5095, Australia;*

[d] *Guangzhou Institute of Geochemistry, Chinese Academy of Sciences, Wushan, Guangzhou 510640, China*

Corresponding Author:

Ray L. Frost

E: r.frost@qut.edu.au

P: +61 7 3138 2407

F: +61 7 3138 1804

• Email address of corresponding author: r.frost@qut.edu.au

Synthesis, characterization of palygorskite supported zero-valent iron and its application for methylene blue decolourisation

Ray L. Frost [a,•], Yunfei Xi [a,b,c], Hongping He [a,d]

[a] *Inorganic Materials Research Program, School of Physical and Chemical Sciences, Queensland University of Technology,GPO Box 2434, 2 George Street, Brisbane, Qld 4001, Australia;*

[b] *CERAR—Centre for Environmental Risk Assessment and Remediation, University of South Australia, Mawson Lakes, SA 5095, Australia;*

[c] *Cooperative Research Centre for Contamination Assessment and Remediation of the Environment (CRC CARE), University of South Australia, Mawson Lakes, SA 5095, Australia;*

[d] *Guangzhou Institute of Geochemistry, Chinese Academy of Sciences, Wushan, Guangzhou 510640, China*

• Email address of corresponding author: r.frost@qut.edu.au

Abstract

In this work, natural palygorskite impregnated with zero-valent iron (ZVI) was prepared and characterised. The combination of ZVI particles on surface of fibrous palygorskite can help to overcome the disadvantage of ultra-fine powders which may have strong tendency to agglomerate into larger particles, resulting in an adverse effect on both effective surface area and catalyst performance. There is a significant increase of methylene blue (MB) decolourized efficiency on acid treated palygorskite with ZVI grafted, within 5 mins, the concentration of MB in the solution was decreased from 94 mg/L to around 20 mg/L and the equilibration was reached at about 30 to 60 mins with only around 10 mg/L MB remained in solution. Changes in the surface and structure of prepared materials were characterized using X-ray diffraction (XRD), infrared (IR) spectroscopy, surface analysing and scanning electron microscopy (SEM) with element analysis and mapping. Comparing with zero-valent iron and palygorskite, the presence of zero-valent iron reactive species on the palygorskite surface strongly increases the decolourization capacity for methylene blue, and it is significant for providing novel modified clay catalyst materials for the removal of organic contaminants from waste water.

Keywords: zero-valent iron, sepiolite, attapulgite, palygorskite, XRD, SEM, EDX, infrared spectroscopy, adsorption-desorption, methylene blue.

1. Introduction

Organic contaminants in the environment especially in water have become a major concern due to their toxicity. To remediate this pollution problem, various chemical, physical and biological processes have been developed, such as microbial degradation, filtration, adsorption, coagulation and membrane separation and others. However, all these remediation methods have suffered from certain limitations and disadvantages such as high cost, poor removal efficiency and possibility of desorption. Thus, in recent years, reactions involving catalytic materials are becoming a more ideal way which will degrade organic contaminants to completely harmless final products. In the last decade, zero-valent iron (ZVI) has been increasingly used in ground water remediation and hazardous waste treatment.

Laboratory studies have demonstrated that ZVI can effectively transform chlorinated solvents, organochlorine pesticides, PCBs, organic dyes and heavy metals [1-5]. These zero-valent iron (ZVI) materials were proposed as a reactive material in permeable reactive barriers (PRBs) due to its great ability in reducing and stabilizing different types of pollutants [6-8]. It has many advantages, such as nontoxic, as iron is abundant in nature, lower price and high activity. This material with particle size at the nano-scale exhibits superior activity because of their larger surface area and higher reactivity [1]. However, similar to other nano-materials, this ultra-fine powder has a strong tendency to agglomerate into larger particles, resulting in an adverse effect on both effective surface area and catalyst performance; while another disadvantage of this material is the separation and recovery of the fine particles after usage. Using a support material for nano-sized ZVI is one possible way to solve this problem. As reported in the literature, there are very few ZVI supported on inorganic clay minerals [9]. Clays as abundant natural resources are suitable candidates to work as supporting materials due to their inexpensiveness, availability, environmental stability and high surface area/sorption capacity and ion exchange properties; their sorption capacity attracts contaminants to the surface and thus enhances the efficiency.

In this study, a PF1-1 palygorskite was investigated as a supporting material for ZVI. This class of clay minerals is characterized by porous crystalline structures containing tetrahedral layers alloyed together by longitudinal side chains [10, 11]. It is

a 2:1 type clay mineral which possesses moderate high structural charge due to considerable substitution of Al^{3+} by Mg^{2+} and Fe^{2+} in the octahedral sheet [12]. In addition, this clay mineral displays fibrous particle shape, fine particle size with internal channels and moderate surface area [13].

A series of tests were carried out to characterise the surface properties of the prepared ZVI materials. In addition, usually ZVI was used for degradation of chlorinated compounds, in this study, this material was extended to methylene blue removal and the removal ability was evaluated in the laboratory. Comparing with ZVI and unmodified palygorskite, palygorskite supported ZVI showed much higher efficiency for methylene blue removal with very small amount of ZVI supported. In this study, scanning electron microscopy (SEM) with EDX together with other characterization methods such as XRD, surface analysing and FTIR have been applied for better understanding of the materials' structures and methylene blue removal mechanisms.

2. Experimental

2.1. Materials

The palygorskite used in this study was supplied by the Clay Minerals Society as source clay PF1-1 (palygorskite). This clay originates from Gadsden County, State of Florida, USA. The chemical composition of the clay is 60.9% SiO_2, 10.4% Al_2O_3, 0.49% TiO_2, 2.98% Fe_2O_3, 0.40% FeO, 0.058% MnO, 10.2% MgO, 1.98% CaO, 0.058% Na_2O, 0.80% K_2O, 0.542% F, 0.80% P_2O_5 and 0.11% S. The formula of the palygorskite can be expressed as $(Ca_{0.12}\ Na_{0.32}\ K_{0.05})\ [Al_{3.01}\ Fe(III)_{0.41}\ Mn_{0.01}\ Mg_{0.54}\ Ti_{0.02}][Si_{7.98}\ Al_{0.02}]O_{20}(OH)_4$, as calculated from its chemical composition. The cation exchange capacity (CEC) is 19.5 meq/100 g and surface area is 136.4 m^2/g. The clay was acid activated using 5M HCl. Sodium borohydride ($NaBH_4$) 98.5%, Iron (II) chloride tetrahydrate ($FeCl_2 \cdot 4H_2O$) 99% and Methylene blue (MB) were obtained from Sigma-Aldrich, absolute ethanol and hydrogen chloride were with analytical grade and used without purification. A reduced iron powder was obtained from Sigma with a purity of 99%.

2.2. Preparation of ZVI and ZVI impregnated palygorskite

10g of Palygorskite was pre-treated by soaking in 200ml of 5M HCl at 60 °C oven for about 48 hrs and then was washed several times with deionized (DI) water to remove excess acid. A liquid phase reduction method was used for nZVI and nZVI impregnated palygorskite. In a typical procedure of ZVI preparation, 16.02 g of $FeCl_2 \cdot 4H_2O$ was dissolved in a mixture of absolute ethanol and de-ionised water (72 ml ethanol plus 18 ml H_2O), this mixture is denoted as solution A. while 9.15g of $NaBH_4$ was dissolved in 300ml of H_2O to form 1M solution, denoted as solution B. Then solution B was added drop by drop to solution A in a fume hood, the resulting reaction can be expressed as $Fe^{2+} + 2BH_4^- + 6H_2O \rightarrow Fe^0 + 2B(OH)_3 + 7H_2\uparrow$, black particles of ZVI appeared and then the mixture was further stirred for 2hrs and the iron powder was separated from the solution by centrifugation and the sediment washed with 250ml ethanol and dried in a 50°C oven without air evacuation overnight. The powder prepared was kept in vacuum desiccator before use. This laboratory made ZVI was denoted as ZVI-L. ZVI impregnated palygorskite was prepared by a similar procedure as reported [9] with following steps: (a) 16.02g of $FeCl_2 \cdot 4H_2O$ was dissolved in mixture of absolute ethanol and deionized (DI) water (72 ml ethanol + 18 ml H_2O), (b) 4.5g of acid treated palygorskite was suspended in the solution, the mixture was stirred using a magnetic stirrer overnight for fully exchange/sorption of iron (II) ions on clay. (c) The mixture was centrifuged and washed several times to remove excess iron (II) ions and then it was resuspended into 72 ml of ethanol + 18 ml H_2O. After that, 300 ml of 1 M borohydride was added drop by drop to the solution and further mixing of 2 hrs was allowed following the addition of $NaBH_4$ solution; then the solid was centrifuged and washed three times with 120 ml of ethanol and dried in 50 °C oven without air evacuation overnight, this palygorskite supported ZVI was denoted as ZVI-P. As reported in the literature, using ethanol to wash samples instead of water is critical in stabilizing ZVI against immediate oxidation [1, 14], and drying in atmosphere oven has a passivation effect for ZVI application which may otherwise catch fire on exposure to atmospheric oxygen [14].

2.3. Characterisation methods

The samples were pressed in stainless steel sample holders. X-ray diffraction (XRD) patterns were recorded using Cu$K\alpha$ radiation (n = 1.5418Å) on a Panalytical X'Pert (PW3040) diffractometer operating at 40 kV and 50 mA between 3 and 73° or 5 to 90° *(2θ)* at a step size of 0.0167°.

Infrared spectra were obtained using a Nicolet Nexus 870 FTIR spectrometer with a smart endurance single bounce diamond ATR cell. Spectra over the 4000–550 cm^{-1} range were obtained by the co-addition of 64 scans with a resolution of 4 cm^{-1} and a mirror velocity of 0.6329 cm/s.

Peakfit software package (AISN Software Inc.) was used to undertake band component analysis that enabled the type of fitting function to be selected and allowed specific parameters to be fixed or varied accordingly. Gauss–Lorentz cross-product function with the minimum number of component bands was used for band fitting. The fitting was undertaken until reproducible results were obtained with squared correlations of r^2 greater than 0.98.

Adsorption and desorption experiments using N_2 were carried out at 77 K on a TRISTAR 3000 surface analyser. Prior to each measurement the samples were degassed at 353K for 24hrs. The N_2 isotherms were used to calculate the specific surface area (SA) and the surface area was determined using multipoint BET method [15]. An FEI QUANTA 200 scanning electron microscope (SEM) with integrated energy dispersive X-ray analyser system was used for morphological studies, samples were coated with carbon. A Philips CM 200 transmission electron microscope (TEM) was used to investigate the microstructure of prepared nZVI.

2.4. Methylene blue decolourization tests

Methylene blue decolourization experiments were conducted at room temperature (25 °C). In a typical experiment, 0.4 g of sample was mixed with 400 ml of 100 ppm methylene blue solution at its natural pH. The solution was stirred for certain period of time using a magnetic stirrer. At certain time intervals, about 4 ml of liquid sample was removed by syringe and filtered using 0.45 μm PTFE syringe filters, dye concentration was determined spectrophotometrically on an Varian Cary 3 UV-Visible Spectrophotometer by measuring absorbance at k_{max} of 665 nm for MB [13]. The change of MB amount was calculated from the difference between the initial and final/equilibrium solution concentrations; solid-phase loading of MB, q_e (mg/g) was computed from the mass balance: $q_e = V(C_i - C_e)/M$; where, C_i and C_e are

total dissolved and equilibrium liquid phase concentration (mg/L), respectively, and M is the dose of sorbent (g/L), V is the volume of the solution (mL). Blank experiments were also performed using solutions without sorbent materials in order to check any possible loss from sorption onto the surface of beaker/syringe/filters and the results showed that the sorption onto surfaces were negligible. All working solutions were prepared from MB stock solution diluted with deionized (DI) water and all experiments were carried out in duplicate.

3. Results and discussion

3.1 Characterization results

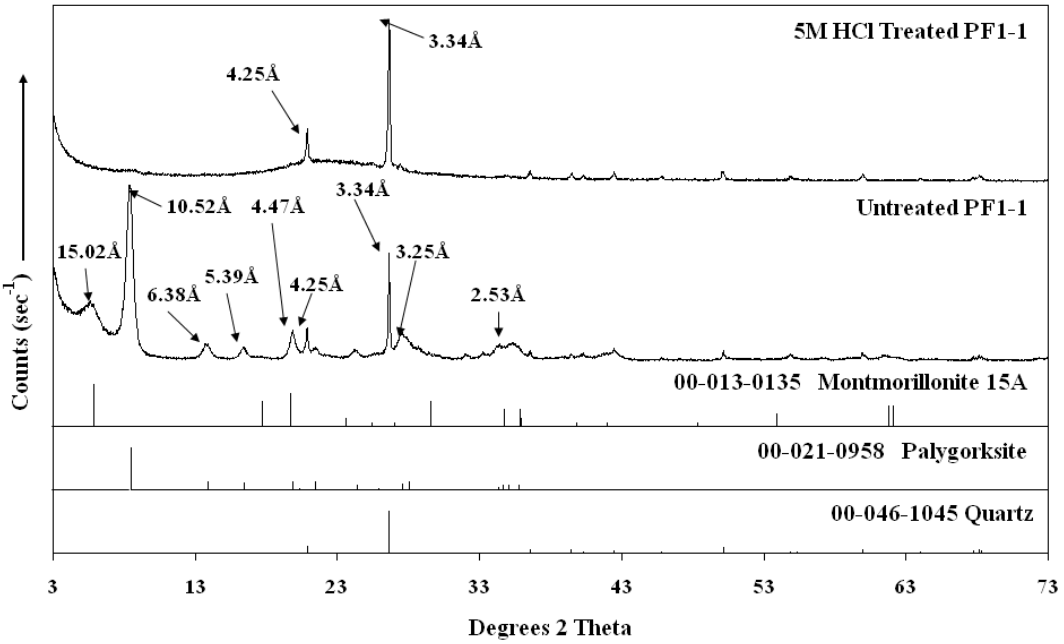

Fig. 1a XRD patterns of untreated/acid treated palygorskite

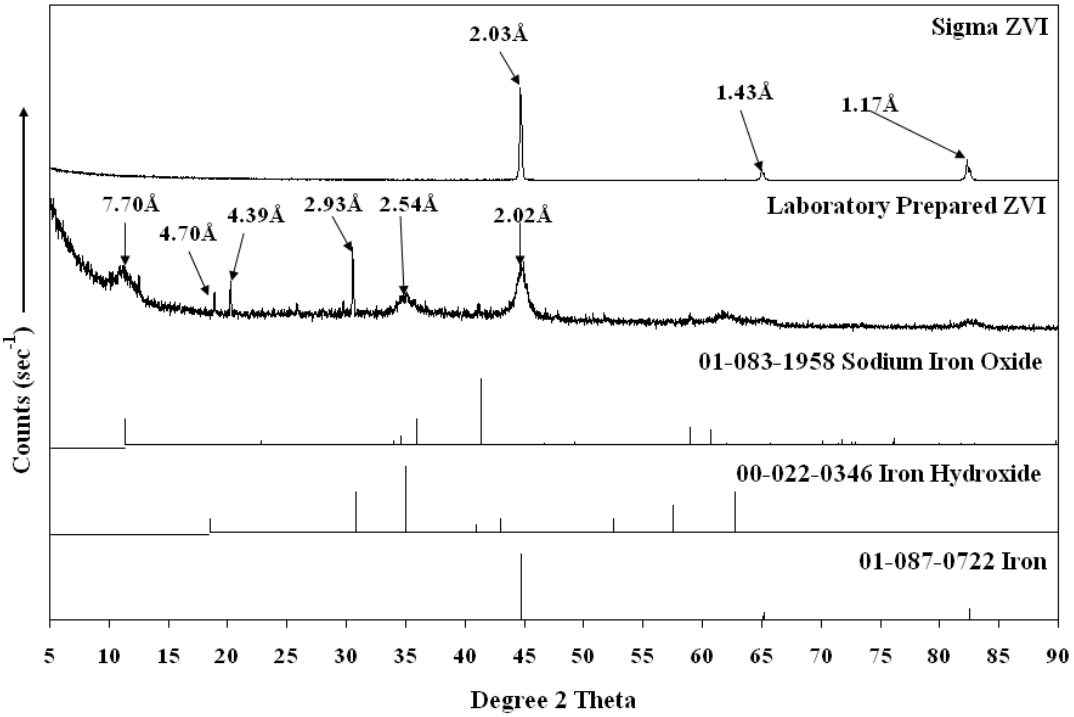

222

223 **Fig. 1b XRD patterns of lab made ZVI and ZVI from Sigma**

224

225

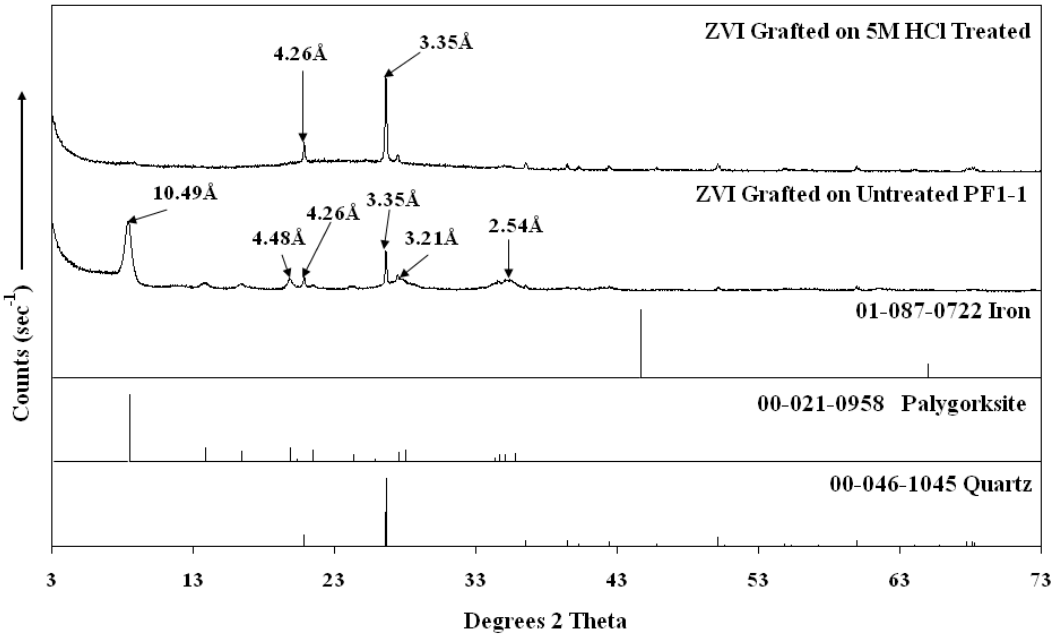

226

227 **Fig. 1c XRD patterns of ZVI grafted on untreated/acid treated palygorskite**

228

229

230

X-ray diffraction

Fig. 1 shows the XRD patterns of untreated palygorskite, 5M HCl treated palygorskite, palygorskite supported ZVI, ZVI from Sigma and laboratory made ZVI. In case of the untreated palygorskite, powder XRD shows peaks that match the pattern in the JCPDS standard 00-021-0958, the peak observed at 10.52 Å is prominent and attributed to the (110) plane which comes from the large distance between neighbour half-unit cells in the crystal structure. In addition, the relatively strong peaks at 4.25 Å, 4.47 Å and 3.69 Å represent the 040, 121 and 221 planes, respectively. While an intense peak at 3.34 Å ($2\theta = 26.7°$) is from a quartz impurity [16]. Other peaks at 6.38 Å, 5.39 Å, 3.25 Å and 2.53 Å were also observed for this PF1-1-palygorskite. After this clay was treated with 5 M HCl, only peak at 4.25 Å and peak from quartz at 3.34 Å were observed. It is concluded that this acid treatment has changed the crystal structure of palygorskite and this palygorskite is less stable under acid attack than another palygorskite the results of which reported in a literature [17]. The XRD patterns of laboratory synthesised ZVI and ZVI obtained from Sigma are shown in Fig. 1b. Both ZVIs showed strong peaks at about 2.02 Å and 2.03 Å respectively which is a characteristic reflection for ZVI [14]. And it also indicates that for ZVI from Sigma, the iron is mainly in its Fe0 state (only characterised by the basic reflection at 44.9° (2θ), however some oxides were observed in laboratory made ZVI which showed peaks at 2.93 Å and 2.54 Å ascribed to lepidocrocite (γ-FeOOH) and magnetite (Fe_3O_4)/ maghemite (γ-Fe_2O_3) respectively. Some researchers have suggested a core-shell structure [18-20], where the iron nanoparticles form a core composed of zero-valent iron with a shell of iron oxides. Because of surface hydroxylation, FeOOH is also present [20]. Small peaks at about 1.43 Å and 1.17 Å were also observed on both samples from iron which is in accordance with that reported in a literature [21]. With ZVI grafted on untreated PF1-1 and 5M HCl treated palygorskite as shown in Fig. 1c, no obvious iron peak at 2.02 Å was observed in both cases and in both samples, the palygorskite peaks were well preserved. The absence of strong iron peak may be due to the smaller amount of ZVI grafted on clays.

Infrared Spectroscopy

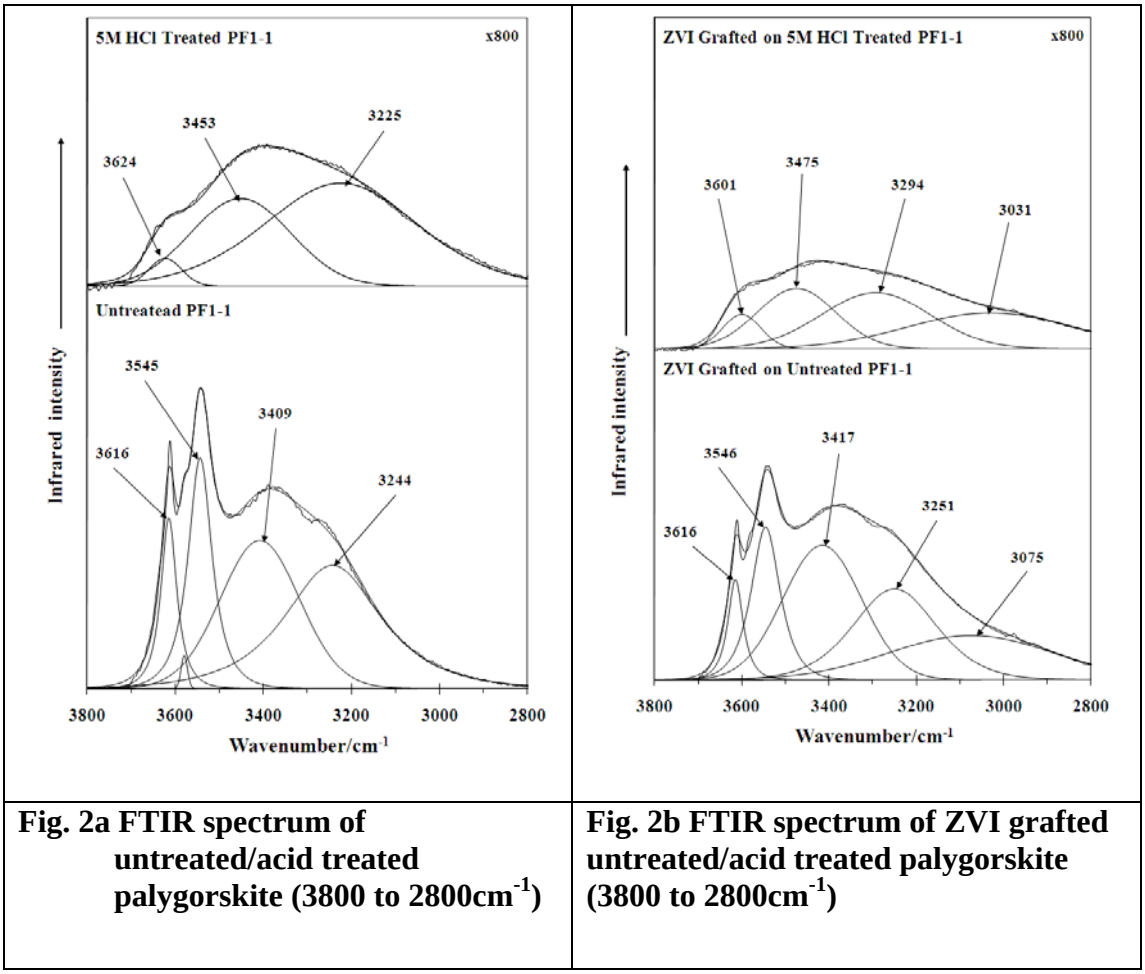

Fig. 2a FTIR spectrum of untreated/acid treated palygorskite (3800 to 2800cm^{-1})

Fig. 2b FTIR spectrum of ZVI grafted untreated/acid treated palygorskite (3800 to 2800cm^{-1})

The infrared spectrum of the palygorskite clay, acid treated palygorskite and ZVI grafted samples may be divided into three sections: (a) 2800-3800 cm^{-1} (Figure 2), (b) 1300-1700 cm^{-1} (Figure 3) and (c) 600-1300 cm^{-1} (Figure 4) for easier study. Fig. 2a shows the OH-stretching vibration region, the following peaks can be observed for untreated palygorskite: sharp peaks at 3616 cm^{-1} and 3545 cm^{-1}, a peak at 3409 cm^{-1} and a shoulder at 3244 cm^{-1}, where the peak at 3616 cm^{-1} is a characteristic peak for palygorskite as described in many studies [22-25], corresponding to Al-Al-OH stretching band. This band shifts to 3624 cm^{-1} with less intensity after acid treatment, a tiny peak was observed at about 3580 cm^{-1} which is ascribed to coordinated water molecules in the channels of the palygorskite [25, 26] or Al-Fe-OH/Al-Mg-OH bonds [25, 27], while band at 3545 cm^{-1} is attributed to OH stretching vibration of water coordinated to Al, Mg [28]. A contribution of the OH stretching mode in Al–Mg–OH, Fe–Mg–OH and Fe-Fe–OH groups is also considered [25, 26].

The bands studied are similar in position and intensity after ZVI grafted on untreated palygorskite as shown in Fig. 2b. However after acid treatment, no matter with ZVI grafted or not, there are big differences of bands' position and intensity in this region as can be observed in Fig. 3a and Fig. 3b.

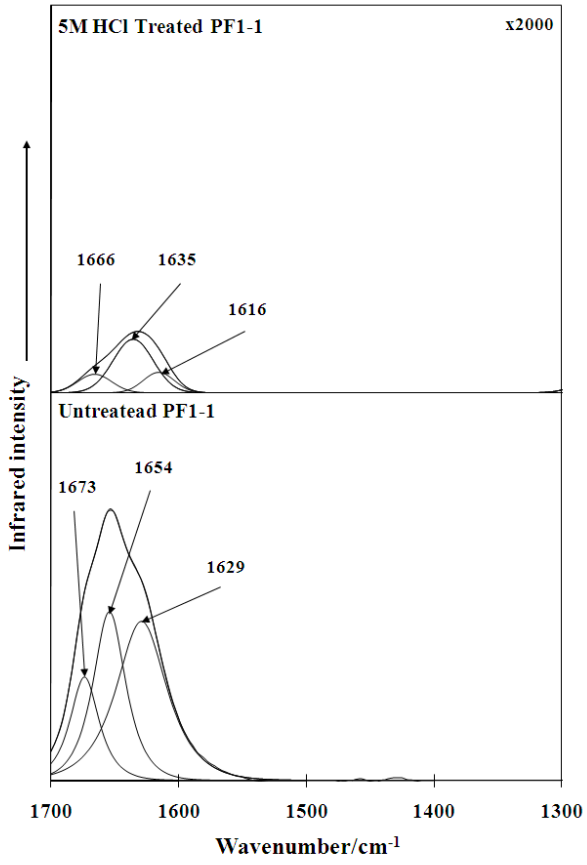

Fig. 3a FTIR spectrum of untreated/acid treated palygorskite (1700 to 1300cm^{-1})

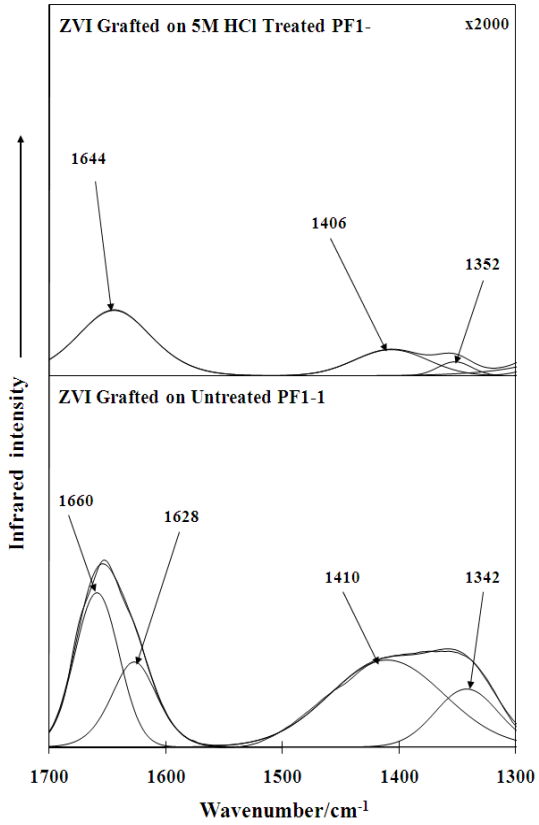

Fig. 3b FTIR spectrum of ZVI grafted untreated/acid treated PF1-1 palygorskite (1700 to 1300cm^{-1})

In the water-bending vibrational region, two partially resolved peaks at 1654 cm^{-1} and 1629 cm^{-1} were observed as shown in Fig. 3a which correspond to bending modes of absorbed and zeolitic water and they are in accordance with the literature [29] which reported the presence of peaks at 1655 cm^{-1} and 1630 cm^{-1} respectively. Though peaks intensities changed significantly, however after acid treatment, the peaks positions in this region didn't change by a great deal. As shown in Fig. 4a, the peaks between 1200 cm^{-1} and 600 cm^{-1} are characteristic bands of silicate corresponding to tetrahedral sheet Si-O stretching modes and M-O deformation [23].

When the spectra of the samples are compared, some important differences can be found as significant differences in the peaks' intensities from untreated and 5M HCl treated palygorskites are observed, after acid treatment the peak intensities in this region was decreased dramatically. The first peak that appears in this region in all samples studied is located at 1194 cm^{-1} which is characteristic of palygorskite. This peak shifts to 1218 cm^{-1} after acid treatment. This peak only appears in palygorskite and sepiolite but not in lamellar clay minerals and is from Si-O-Si bond [24] between the alternative ribbons.

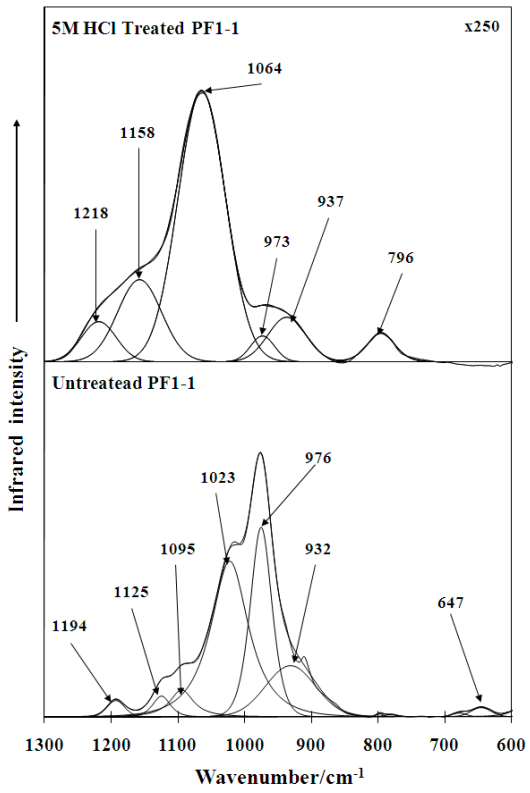

Fig. 4a FTIR spectrum of untreated/acid treated palygorskite (1300 to 600cm^{-1})

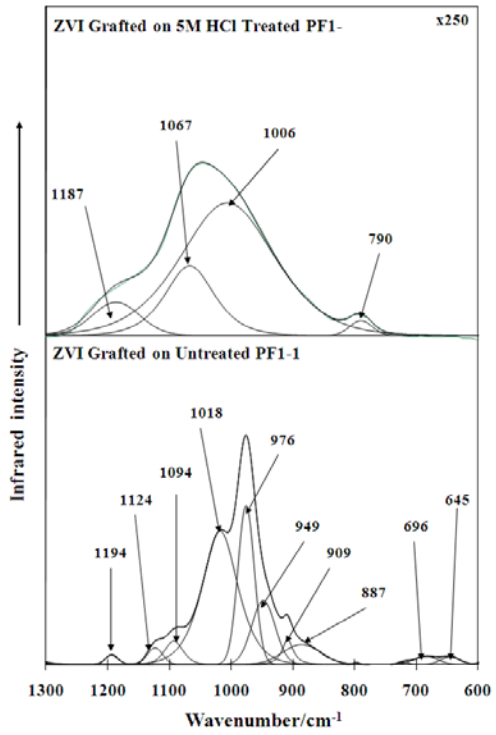

Fig. 4b FTIR spectrum of ZVI grafted on untreated/acid treated PF1-1 palygorskite (1300 to 600cm^{-1})

The most intensive peaks observed in this region are at 1023 cm^{-1} and 976 cm^{-1} respectively corresponding to stretching vibration of Si-O bond [30]. There are changes observed on these bands after acid treatment which may due to the dissolution of octahedral sheets, where the silicate sheets presumably convert to silanol groups [24]. The presence of small quantities of impurities can be clearly

detected in this spectrum, where quartz produced band at about 796 cm^{-1} [25, 28] and this peak became relative stronger comparing with other peaks in this region after acid treatment which showed quartz was resistance to acid treatment, and it also confirmed the conclusion as obtained from XRD results. There are also several other bands observed where one placed at about 647 cm^{-1} are related to bonds corresponding to tetrahedral sheet. The shoulder at 676 cm^{-1} is related to the Mg content, after acid treatment, these bands are not observed, which may due to the loss of Mg contents after acid washing. And acid treated palygorskite showed quite some difference in peaks position and intensity comparing with untreated one.

BET adsorption-desorption

Adsorption and desorption experiments using N_2 were carried out at 77 K. The N_2 isotherms have been applied to calculate the specific surface area (SA) using multipoint BET [15] method. It can be observed that acid treatment has increased the surface area of palygorskite from 209.88 m^2/g to 277.62 m^2/g which is in accordance with conclusion drawn in a literature [17]. And in literature, acid treatment showed increased number of sorption sites toward metal ions on palygorskite, as this procedure may disaggregate particles, eliminate impurities and increase surface area of the clay [10, 31]. It also leads to partial leaching of magnesium, aluminium and iron contents of palygorskite [32]. Preliminary results have shown that ZVI grafted on acid treated palygorskite has better reactivity compared with grafted on untreated clay (results not shown). ZVI purchased from Sigma only has a surface area at about 0.12 m^2/g, however laboratory prepared ZVI showed a surface area at 80.6 m^2/g. It was also observed that after ZVI grafting on acid treated palygorskite, the surface area decreased from 277.6 m^2/g to 76.9 m^2/g.

344 **Scanning electron microscopy**

345

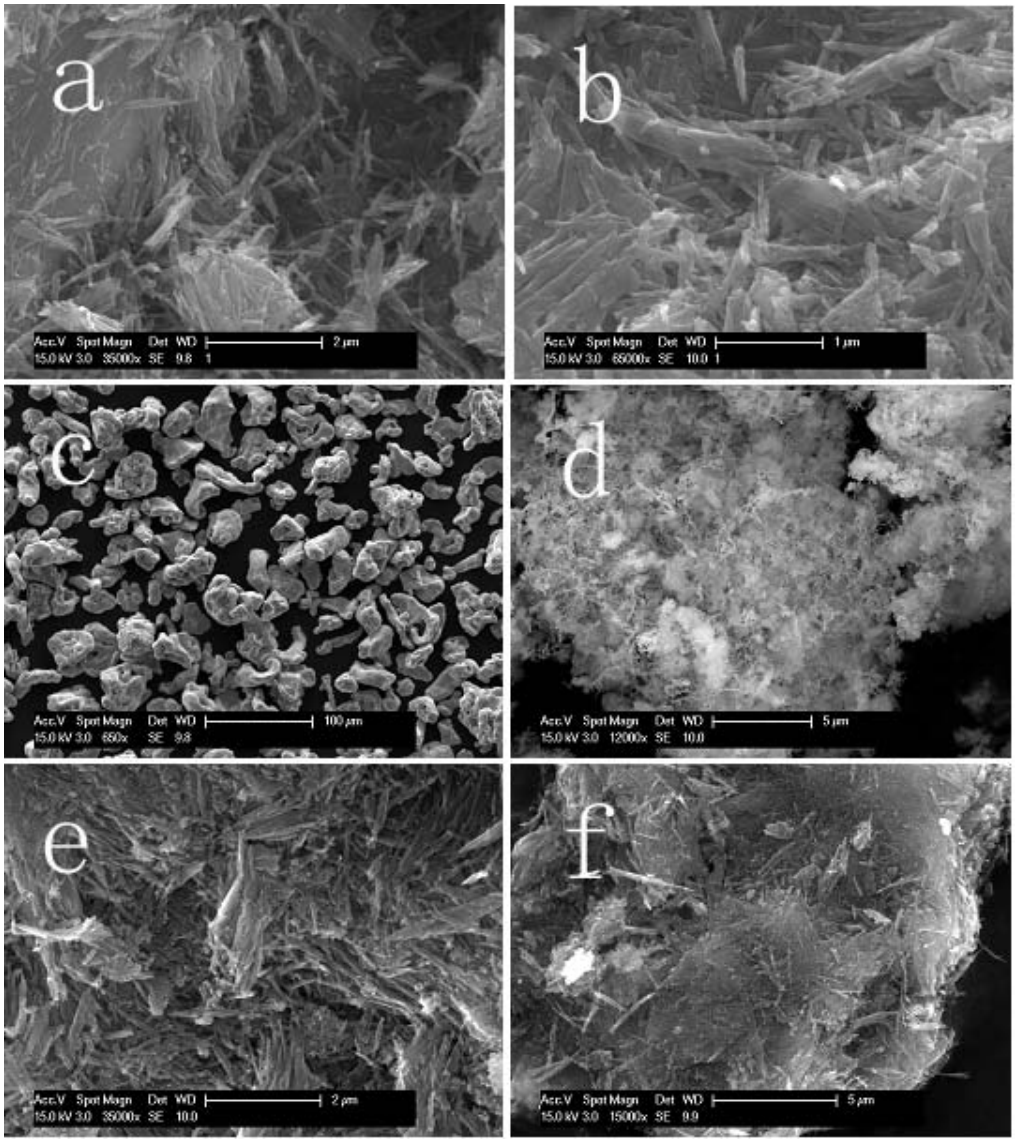

346

347 **Fig. 5 SEM images of a: untreated PF1-1 palygorskite; b: 5M HCl treated**
348 **palygorskite; c: ZVI from Sigma; d: laboratory made ZVI; e: ZVI grafted on**
349 **treated palygorskite and f: ZVI grafted on untreated palygorskite**

350

351 The SEM images of the pakygorskite and its modified products are shown in
352 Figure 5. The unmodified palygorskite (Fig. 5a) shows bundles of close packed fibres
353 [33] or mat of tightly interwoven fibres [34], with variable thickness and length.
354 These fibres have flat or straight shapes and are oriented randomly in aggregates
355 similar to that observed in some other studies [11, 35]. Morphologic differences
356 between unmodified palygorskite and ZVI grafted palygorskite are not significant and
357 only textural features were observed on the surface of the clay which may due to the

iron particles after ZVI grafting. The SEM images of Sigma ZVI and laboratory prepared ZVI are shown in Fig. 5c and 5d. The ZVI obtained from Sigma showed big particles with sizes at around several tens of microns with irregular shapes (Fig. 5c). The laboratory made iron particles (Fig. 5d) demonstrate the chain-like morphology with floc aggregates similar to that observed in a study [1]. The morphology and size difference of two kinds of ZVIs also illustrated the big differences on surface areas obtained as discussed above. It is also likely that the ZVI has core-shell structures where oxidised irons surround Fe(0) core and thus prevent it against further oxidation. SEM in this study is also used to examine the changes in morphology of palygorskite upon modification with ZVI.

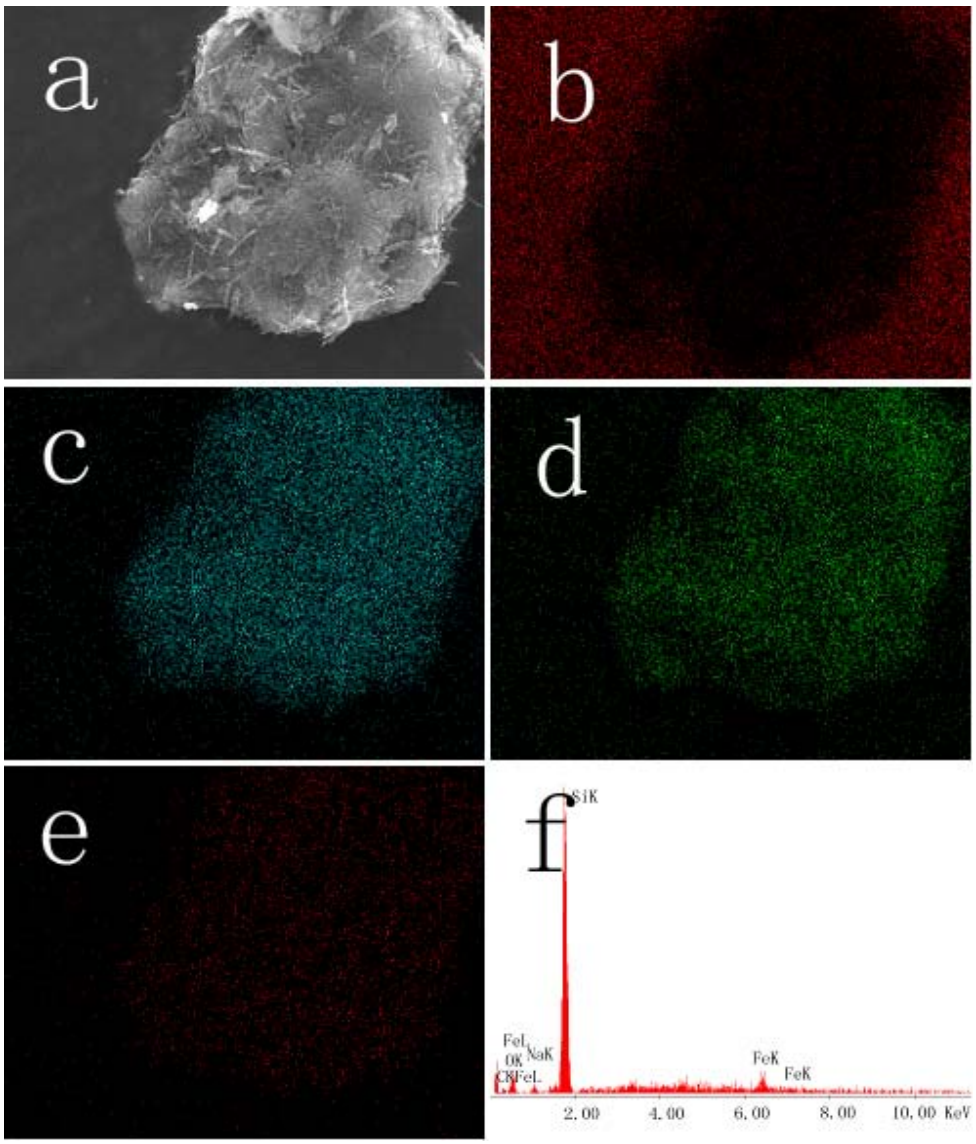

Fig. 6 EDX mapping and element analysis on ZVI grafted palygorskite a: SEM image; b: C element distribution; c: Si element distribution; d: O element distribution; e: Fe element distribution and f: EDX spectrum of selected area

EDX mapping and element analysis are shown in Figure 6. EDX element analysing has demonstrated that after acid treatment, fewer amounts of magnesium and aluminium were observed as shown in Fig. 6f, and a tiny peak from Fe was shown in this figure which proves the successful grafting of ZVI on palygorskite surface, and this peak was not observed in acid treated sample (figure not shown). The EDX mappings of elements C, Si, O and Fe in a selected area of ZVI grafted palygorskite are illustrated in Fig. 6b, Fig. 6c, Fig. 6d and Fig. 6e respectively where even distribution of elements including Fe are present. This observation has also confirmed the grafting of ZVI on clay surface. It is observed in TEM (Fig. 7) that the chain-like laboratory made nZVI is composed of sphere shaped (but not regular) particles as basic units, these ZVI particles have a size at around 80 nm in diameter.

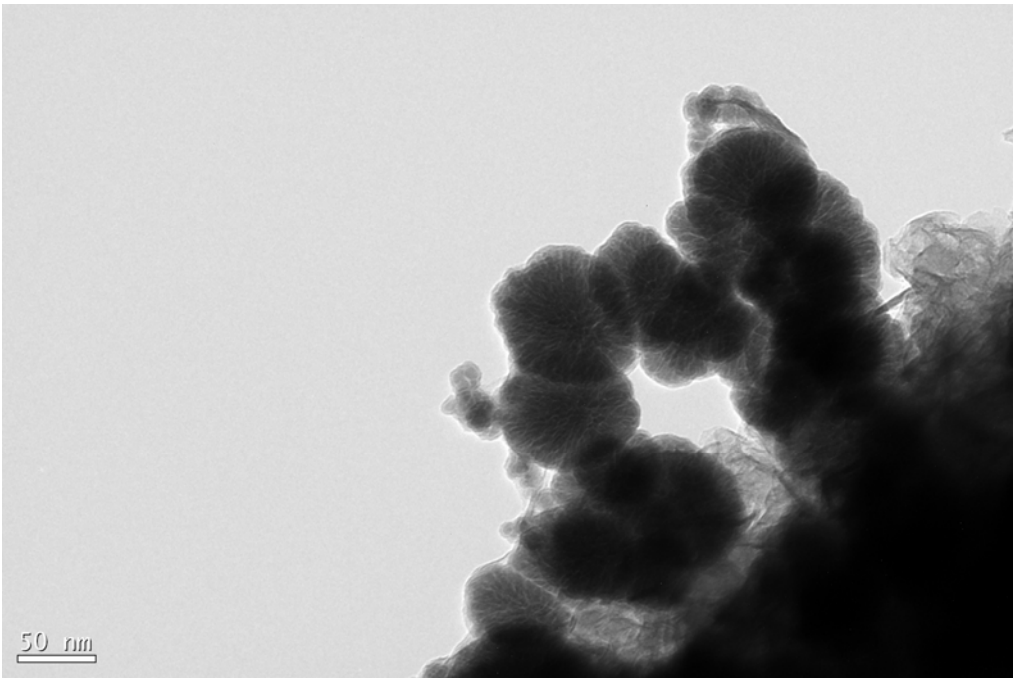

Fig. 7 TEM image of laboratory made ZVI particles

3.2 MB decolourization results

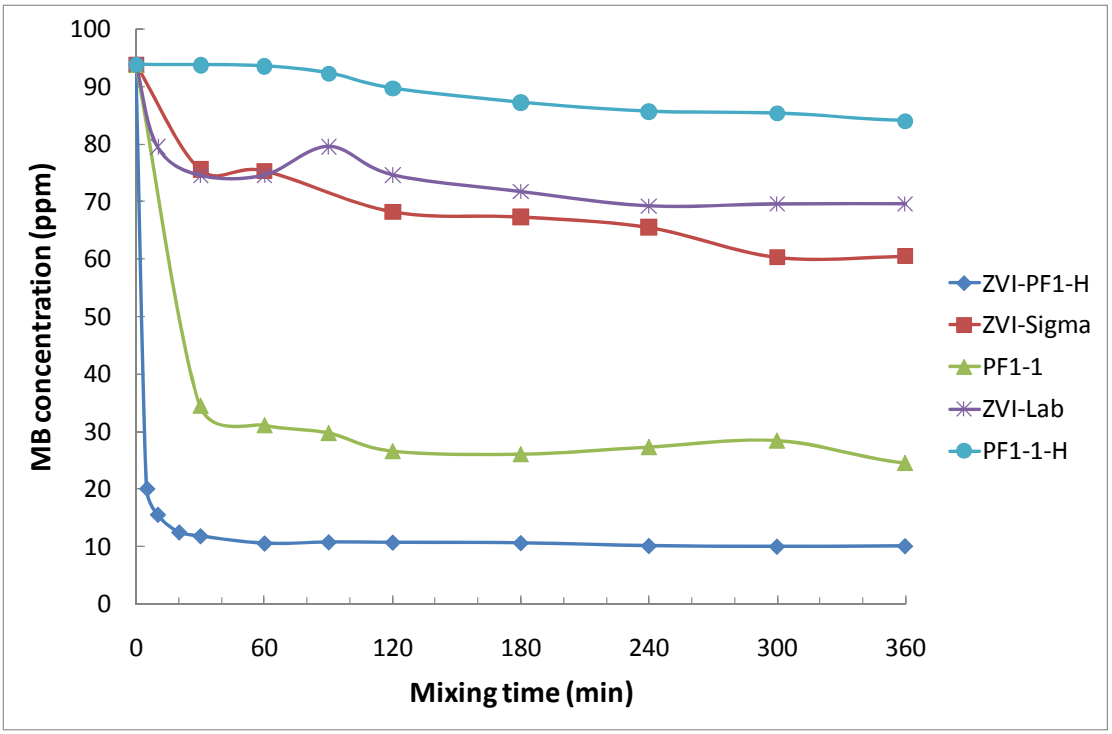

Fig. 7 Effect of mixing time on MB removal

For optimising decolourization time, at natural pH of 5.9, a set of experiments has been performed equilibrating 400 mL of approximate 100 mg/L MB solution with 0.4 g of different materials. The suspensions were usually shaken at 25 °C for certain period of time (5, 10, 30, 60, 90, 120, 180, 240, 300mins and up to 360mins), then the dye concentration has been measured to calculate MB concentration remained in solution. Fig. 8 shows the time dependent MB decolourization curve for all the investigated samples. It can be seen that among all the samples, acid treated palygorskite can absorb least amount of MB and within the first 60 mins, only negligible amount was adsorbed. Even up to 360 mins, the concentration of MB was only decreased from 94 mg/L to 84 mg/L (10.4% absorbed), and its performance is even worse comparing with that of unmodified palygorskite where there is an obvious decrease of MB concentration within 30 mins with 34.5 mg/L left in the solution and afterwards the concentration was further decreased to about 24-26 mg/L, this demonstrates that MB which has positive charged groups can be absorbed by negatively charged clay surface. As for laboratory made ZVI and ZVI obtained from Sigma, with increase of contact time, the amount of MB removed was increased steadily and the decolourization capacities for both samples are comparable and concentrations lower than 75 mg/L was reached within 30 mins and then it was

decreased to 69-60 mg/L until 360 mins of contact time. Generally, lab made ZVI can decolour slightly higher amount of MB than that purchased from Sigma, it may because lab made ZVI has much higher surface area at about 80.6 m^2/g comparing with that obtained from Sigma with a surface area only at 0.12 m^2/g, the morphology differences between these two ZVIs are also the possible reason to interpret the higher activity obtained on lab made ZVI.

There is a significant increase of MB decolourized efficiency on acid treated palygorskite with ZVI grafted, within 5 mins, the concentration of MB in the solution was decreased from 94 mg/L to around 20 mg/L and the equilibration was reached at about 30 to 60 mins with only around 10 mg/L MB remained in the solution. It is apparent that modification of palygorskite with ZVI can increase the sorption capacity comparing with only ZVI or palygorskite. The decolourization mechanism can be the reduction of MB to leukomethylene blue (LMB) by ZVI species and the adsorption of MB directly on ZVI surface, but as ZVI grafted palygorskite showed better results comparing with ZVI only, adsorption of MB may not be the most important factor. But it is more likely that co-precipitation with in-situ generated corrosion products can be the main reason which could interpret the uptake of MB from solution as discussed in some studies [36]. And the Fe(0) on clay surface could corrode more rapidly, especially when these particles are well distributed on the surface of acid activated palygorskite, thereby showed significant higher activity in the MB decolourization than only on ZVI or clay. Further work will be needed to optimize the MB decolourization procedure.

4. Conclusions

Zero valent iron (ZVI) and ZVI grafted palygorskite were prepared using reduction methods and these materials together with untreated/acid treated palygorskite, ZVI purchased from Sigma have been applied for methylene blue decolourization. It was observed that ZVI grafted palygorskite has increased decolourization capacity on MB comparing with that of ZVI or untreated palygorskite, and co-precipitation on in-situ generated corrosion iron products was probably the main reason explaining the uptake of MB from the studied solutions. In this study, X-ray diffraction patterns were obtained for these materials; peaks from different planes

diffractions were illuminated and quartz was determined as a main impurity, it was observed that the acid treatment has changed the crystal structure of palygorskite. Comparing with ZVI obtained from Sigma which has mainly iron phase, laboratory made ZVI showed phases from iron oxides. SEM studies showed different morphology between these two ZVIs, the structural information of palygorskite and ZVI grafted ones were also obtained and discussed. EDX element mapping was proven to be a useful tool illustrating the distribution of elements, and iron phase though not detected by XRD, was observed evenly distributed on the clay surface by this technique. Infrared ATR techniques were used to study the changes in the bands positions of palygorskite upon acid treatment and ZVI grafting, changes in both the wavenumber and the intensity of the bands were observed after acid treatment and grafting. The result is very important for the application of ZVI grafted natural clays for the decolourization of organic dyes from waste water.

Acknowledgements

The financial and infra-structure support of the Queensland University of Technology Inorganic Materials Research Program of the School of Physical and Chemical Sciences is gratefully acknowledged. The Australian Research Council (ARC) is thanked for funding the instrumentation

References

1. C. Uzum, et al., *Application of zero-valent iron nanoparticles for the removal of aqueous Co2+ ions under various experimental conditions.* Chemical Engineering Journal, 2008. **144**(2): p. 213-220.
2. Cantrell, K.J., D.I. Kaplan, and T.W. Wietsma, *Zero-valent iron for the in situ remediation of selected metals in groundwater.* Journal of Hazardous Materials, 1995. **42**(2): p. 201-212.
3. Cho, H.-H. and J.-W. Park, *Sorption and reduction of tetrachloroethylene with zero valent iron and amphiphilic molecules.* Chemosphere, 2006. **64**(6): p. 1047-1052.
4. Dombek, T., et al., *Rapid reductive dechlorination of atrazine by zero-valent iron under acidic conditions.* Environmental Pollution, 2001. **111**(1): p. 21-27.

5. Ghauch, A., et al., *Rapid treatment of water contamined with atrazine and parathion with zero-valent iron.* Chemosphere, 1999. **39**(8): p. 1309-1315.
6. Scherer, M.M., et al., *Chemistry and Microbiology of Permeable Reactive Barriers for In Situ Groundwater Clean up.* Critical Reviews in Environmental Science and Technology, 2000. **30**(3): p. 363-411.
7. Cundy, A.B., L. Hopkinson, and R.L.D. Whitby, *Use of iron-based technologies in contaminated land and groundwater remediation: A review.* Science of The Total Environment. **In Press, Corrected Proof**.
8. Ahn, J.S., et al., *Arsenic removal using steel manufacturing byproducts as permeable reactive materials in mine tailing containment systems.* Water Research, 2003. **37**(10): p. 2478-2488.
9. Uzum, C., et al., *Synthesis and characterization of kaolinite-supported zero-valent iron nanoparticles and their application for the removal of aqueous Cu2+ and Co2+ ions.* Applied Clay Science. **In Press, Corrected Proof**.
10. Chen, H., Y. Zhao, and A. Wang, *Removal of Cu(II) from aqueous solution by adsorption onto acid-activated palygorskite.* Journal of Hazardous Materials, 2007. **149**(2): p. 346-354.
11. Aiban, S.A., *Compressibility and swelling characteristics of Al-Khobar Palygorskite, eastern Saudi Arabia.* Engineering Geology, 2006. **87**(3-4): p. 205-219.
12. Polette-Niewold, L.A., et al., *Organic/inorganic complex pigments: Ancient colors Maya Blue.* Journal of Inorganic Biochemistry, 2007. **101**(11-12): p. 1958-1973.
13. Al-Futaisi, A., A. Jamrah, and R. Al-Hanai, *Aspects of cationic dye molecule adsorption to palygorskite.* Desalination, 2007. **214**(1-3): p. 327-342.
14. Celebi, O., et al., *A radiotracer study of the adsorption behavior of aqueous Ba2+ ions on nanoparticles of zero-valent iron.* Journal of Hazardous Materials, 2007. **148**(3): p. 761-767.
15. Brunauer, S., P.H. Emmett, and E. Teller, *Adsorption of gases in multimolecular layers.* Journal of the American Chemical Society, 1938. **60**: p. 309-19.
16. Post, J.L. and S. Crawford, *Varied forms of palygorskite and sepiolite from different geologic systems.* Applied Clay Science, 2007. **36**(4): p. 232-244.

17. Corma, A., A. Mifsud, and E. Sanz, *Influence of the chemical composition and textural characteristics of palygorskite on the acid leaching of octahedral cations.* Clay Minerals, 1987. **22**(2): p. 225-32.
18. Nurmi, J.T., et al., *Characterization and Properties of Metallic Iron Nanoparticles: Spectroscopy, Electrochemistry, and Kinetics.* Environmental Science and Technology, 2005. **39**(5): p. 1221-1230.
19. Liu, Y., et al., *Trichloroethene Hydrodechlorination in Water by Highly Disordered Monometallic Nanoiron.* Chemistry of Materials, 2005. **17**(21): p. 5315-5322.
20. Sun, Y.-P., et al., *Characterization of zero-valent iron nanoparticles.* Advances in Colloid and Interface Science, 2006. **120**(1-3): p. 47-56.
21. Chen, L.-H., C.-C. Huang, and H.-L. Lien, *Bimetallic iron-aluminum particles for dechlorination of carbon tetrachloride.* Chemosphere, 2008. **73**(5): p. 692-697.
22. Frost, R.L., G.A. Cash, and J.T. Kloprogge, *[`]Rocky Mountain leather', sepiolite and attapulgite--an infrared emission spectroscopic study.* Vibrational Spectroscopy, 1998. **16**(2): p. 173-184.
23. Frost, R.L., et al., *Near-infrared and mid-infrared spectroscopic study of sepiolites and palygorskites.* Vibrational Spectroscopy, 2001. **27**(1): p. 1-13.
24. McKeown, D.A., J.E. Post, and E.S. Etz, *Vibrational analysis of palygorskite and sepiolite.* Clays Clay Miner. FIELD Full Journal Title:Clays and Clay Minerals, 2002. **50**(5): p. 667-680.
25. Suarez, M. and E. Garcia-Romero, *FTIR spectroscopic study of palygorskite: Influence of the composition of the octahedral sheet.* Applied Clay Science, 2006. **31**(1-2): p. 154-163.
26. Augsburger, M.S., et al., *FTIR and Mossbauer investigation of a substituted palygorskite: Silicate with a channel structure.* Journal of Physics and Chemistry of Solids, 1998. **59**(2): p. 175-180.
27. Chahi, A., S. Petit, and A. Decarreau, *Infrared evidence of dioctahedral-trioctahedral site occupancy in palygorskite.* Clays and Clay Minerals, 2002. **50**(3): p. 306-313.
28. Madejova, J. and P. Komadel, *Baseline studies of the Clay Minerals Society source clays: infrared methods.* Clays and Clay Minerals, 2001. **49**(5): p. 410-432.

29. Mendelovici, E. and D.C. Portillo, *Organic derivatives of attapulgite. I. Infrared spectroscopy and x-ray diffraction studies.* Clays and Clay Minerals, Proceedings of the Conference, 1976. **24**(4): p. 177-82.
30. Blanco, C., et al., *Differences between one aluminic palygorskite and another magnesic by infrared spectroscopy.* Spectroscopy Letters, 1989. **22**(6): p. 659-73.
31. Wang, W., H. Chen, and A. Wang, *Adsorption characteristics of Cd(II) from aqueous solution onto activated palygorskite.* Separation and Purification Technology, 2007. **55**(2): p. 157-164.
32. Jozefaciuk, G. and G. Bowanko, *Effect of acid and alkali treatments on surface areas and adsorption energies of selected minerals.* Clays and Clay Minerals, 2002. **50**(6): p. 771-783.
33. Neaman, A. and A. Singer, *Rheological properties of aqueous suspensions of palygorskite.* Soil Science Society of America Journal, 2000. **64**(1): p. 427-436.
34. Cagatay, M.N., *Palygorskite in the Eocene rocks of the Dammam Dome, Saudi Arabia.* Clays and Clay Minerals, 1990. **38**(3): p. 299-307.
35. Soong, R., *Palygorskite occurrence in northwest Nelson, South Island, New Zealand.* New Zealand Journal of Geology and Geophysics, 1992. **35**(3): p. 325-30.
36. Noubactep, C., *A critical review on the process of contaminant removal in Fe0-H2O systems.* Environmental Technology, 2008. **29**(8): p. 909-920.

List of figures

614

615

616